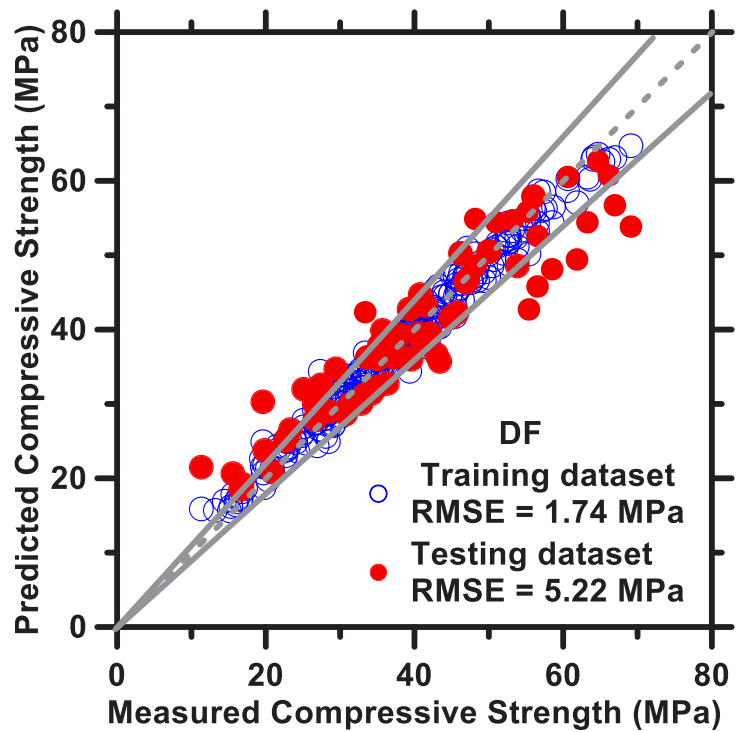
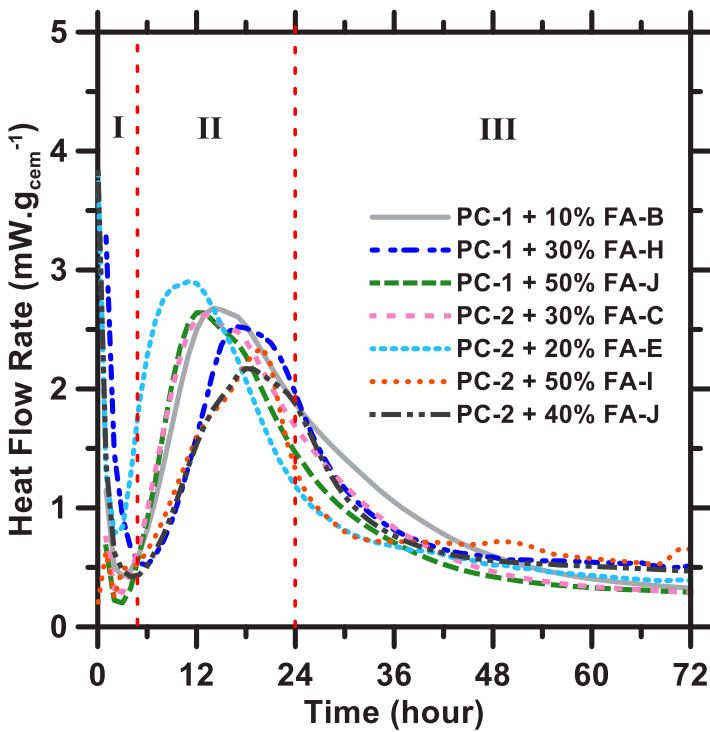


Exploratory Advanced Research Program

Physically Informed Data-Driven Methods for Greatly Enhancing the Use of Heterogeneous Supplementary Cementitious Materials in Transportation Infrastructure

Research Summary Report



Notice

This document is disseminated under the sponsorship of the U.S. Department of Transportation in the interest of information exchange. The U.S. Government assumes no liability for the use of the information contained in this document. This report does not constitute a standard, specification, or regulation.

The U.S. Government does not endorse products or manufacturers. Trademarks or manufacturers' names appear in this document only because they are considered essential to the objective of the document.

Quality Assurance Statement

The Federal Highway Administration (FHWA) provides high-quality information to serve Government, industry, and the public in a manner that promotes public understanding. Standards and policies are used to ensure and maximize the quality, objectivity, utility, and integrity of its information. FHWA periodically reviews quality issues and adjusts its programs and processes to ensure continuous quality improvement.

Recommended citation: Federal Highway Administration, *Physically Informed Data-Driven Methods for Greatly Enhancing the Use of Heterogeneous Supplementary Cementitious Materials in Transportation Infrastructure* (Washington, DC: 2023) <https://doi.org/10.21949/1521984>

Cover image credit:
© 2022 Missouri University of Science and Technology.

1. Report No. FHWA-HRT-23-040	2. Government Accession No.	3. Recipient's Catalog No.	
4. Title and Subtitle Physically Informed Data-Driven Methods for Greatly Enhancing the Use of Heterogeneous Supplementary Cementitious Materials in Transportation Infrastructure		5. Report Date July 2023	
		6. Performing Organization Code	
7. Author(s) G. Sant (ORCID: 0000-0002-1124-5498), M. Bauchy (ORCID: 0000-0003-4600-0631), N. Neithalath (ORCID: 0000-0002-3174-0402), A. Kumar (ORCID: 0000-0001-7550-8034)		8. Performing Organization Report No.	
9. Performing Organization Name and Address University of California, Los Angeles Department of Civil and Environmental Engineering 420 Westwood Plaza, 5731-J Boelter Hall Los Angeles, CA 90095 Schatz Publishing Group 11950 W. Highland Ave. Blackwell, OK 74631		10. Work Unit No.	
		11. Contract or Grant No. 693JJ3-19-50021	
12. Sponsoring Agency Name and Address Office of Corporate Research, Technology, and Innovation Management Federal Highway Administration 6300 Georgetown Pike McLean, VA 22101-2296		13. Type of Report and Period Covered Research Summary Report September 2019–August 2022	
		14. Sponsoring Agency Code HRTM-30	
15. Supplementary Notes The Contracting Officer's representative is Jack Youtcheff (HRDI-10).			
16. Abstract This summary report shares the findings of an Exploratory Advanced Research Program project that investigated strategies for expanding the use of fly ash (FA) in concrete production. With an unprecedented massive concrete and FA dataset collection of 40,000 data records, the team conducted a series of experiments that used advanced material characterizations, machine-learning techniques, and numerical simulations to uncover the fundamental attributes governing the reactivity of FA and its suitability as an ordinary portland cement replacement. This work aimed to enhance the use of FA for producing more sustainable concrete.			
17. Key Words Fly ash, reactivity, supplementary cementitious materials, concrete production, machine learning, topological constraint theory		18. Distribution Statement No restrictions. This document is available to the public through the National Technical Information Service, Springfield, VA 22161. https://www.ntis.gov	
19. Security Classif. (of this report) Unclassified	20. Security Classif. (of this page) Unclassified	21. No. of Pages 10	22. Price N/A

Form DOT F 1700.7 (8-72)

Reproduction of completed page authorized.

SI* (MODERN METRIC) CONVERSION FACTORS				
APPROXIMATE CONVERSIONS TO SI UNITS				
Symbol	When You Know	Multiply By	To Find	Symbol
LENGTH				
in	inches	25.4	millimeters	mm
ft	feet	0.305	meters	m
yd	yards	0.914	meters	m
mi	miles	1.61	kilometers	km
AREA				
in ²	square inches	645.2	square millimeters	mm ²
ft ²	square feet	0.093	square meters	m ²
yd ²	square yard	0.836	square meters	m ²
ac	acres	0.405	hectares	ha
mi ²	square miles	2.59	square kilometers	km ²
VOLUME				
fl oz	fluid ounces	29.57	milliliters	mL
gal	gallons	3.785	liters	L
ft ³	cubic feet	0.028	cubic meters	m ³
yd ³	cubic yards	0.755	cubic meters	m ³
NOTE: volumes greater than 1,000 L shall be shown in m ³				
MASS				
ounces		28.35	grams	g
pounds		0.454	kilograms	kg
short tons (2,000 lb)		0.907	megagrams (or "metric ton")	Mg (or "t")
TEMPERATURE (exact degrees)				
°F	Fahrenheit	5 (F-32)/9 or (F-32)/1.8	Celsius	°C
ILLUMINATION				
foot-candles		10.76	lux	lx
foot-Lamberts		3.426	candela/m ²	cd/m ²
FORCE and PRESSURE or STRESS				
poundforce		4.45	newtons	N
poundforce per square inch		6.89	kilopascals	kPa

APPROXIMATE CONVERSIONS TO SI UNITS				
Symbol	When You Know	Multiply By	To Find	Symbol
LENGTH				
mm	millimeters	0.039	inches	in
m	meters	3.28	feet	ft
m	meters	1.09	yards	yd
km	kilometers	0.621	miles	mi
AREA				
mm ²	square millimeters	0.0016	square inches	in ²
m ²	square meters	10.764	square feet	ft ²
m ²	square meters	1.195	square yards	yd ²
ha	hectares	2.47	acres	ac
km ²	square kilometers	0.386	square miles	mi ²
VOLUME				
mL	milliliters	0.034	fluid ounces	fl oz
L	liters	0.264	gallons	gal
m ³	cubic meters	35.314	cubic feet	ft ³
m ³	cubic meters	1.307	cubic yards	yd ³
MASS				
g	grams	0.035	ounces	oz
kg	kilograms	2.202	pounds	lb
Mg (or "t")	megagrams (or "metric ton")	1.103	short tons (2000 lbs)	T
TEMPERATURE (exact degrees)				
°C	Celsius	1.8C+32	Fahrenheit	°F
ILLUMINATION				
lx	lux	0.0929	foot-candles	fc
cd/m ²	candela/m ²	0.2919	foot-Lamberts	fl
FORCE and PRESSURE or STRESS				
N	newtons	2.225	poundforce	lbf
kPa	kilopascals	0.145	poundforce per square inch	lbfin ²

*SI is the symbol for international System of Units. Appropriate rounding should be made to comply with Section 4 of ASTM E380. (revised March 2003)

Contents

Introduction	1
Project Overview	2
Selecting and Characterizing Physical/Chemical Indicators for the Reactivity of FA	2
Develop Experimental and Synthetic Datasets to Train ML Models to Predict the Engineering Properties of [PC + FA] Mixtures	3
Develop a Set of ML Models to Optimize and Predict the Performance of [PC + FA] Mixtures	6
Predicting Concrete's Strength by ML Balance Between Accuracy and Complexity of Algorithms	6
Using ML to Predict Concrete's Strength: Learning from Small Datasets	7
Interpreting the Strength Activity Index (SAI) of FA with ML	8
Conclusions	9
References	10

LIST OF FIGURES

Figure 1. Schematic. Proposed ML-based screening approach.	3
Figure 2. Graph. Heat-flow rate profiles of randomly selected [PC+ FA] binders.	4
Figure 3. Graph. The standalone DF model predictions of heat-flow rate.	5
Figure 4. Graph. The predictions of compressive strength of [PC+ FA] binders as produced by the DF model against the testing dataset.	6
Figure 5. Graph. Permutation importance of each of the features considered.	7

LIST OF TABLES

Table 1. Statistical parameters pertaining to the prediction performance of DF and [DF + Segmentation] models on 72-h heat-flow rate.	5
Table 2. The statistical parameters pertaining to the prediction performance of the DF and analytical models on [PC+ FA] binders' compressive strength.	6

LIST OF ABBREVIATIONS

AEA	air-entraining admixture	ML	machine learning
ANN	artificial neural network	PC	portland cement
Ca	calcium	R	Pearson correlation coefficient
CAS	calcium aluminosilicate	R²	coefficient of determination
CO₂	carbon dioxide	RMSE	root mean squared error
DF	deep forest	SCM	supplementary cementitious materials
EAR	exploratory advanced research	TCT	topological constraint theory
FA	fly ash	WRA	water-reducing admixture
MAE	mean absolute error	XRF	x-ray fluorescence
MAPE	mean absolute percentage error		

Concrete is the dominant material used in the construction of buildings and infrastructure.⁽¹⁾ However, the production of ordinary portland cement (PC) is associated with substantial carbon dioxide (CO₂) emissions, estimated at nearly 9 percent of the global CO₂ emissions.⁽²⁾ As a result, the industry has sought to replace PC in concrete with supplementary cementitious materials (SCMs). Fly ash (FA), a residue from coal combustion, is currently the only SCM available in sufficient abundance to replace PC in concrete.⁽³⁾ However, FA's diverse chemical composition and the presence of glassy and crystalline phases can make it difficult to use in concrete production. Although it is defined as either Class C or F, the specific composition of a certain FA can greatly affect the performance of the concrete with which it is mixed. Even similar FAs can result in vastly different concrete behavior. As a result, over the past decades, FA has only been used to replace a limited amount of PC in concrete (e.g., ≤25 percent by mass) because it has had limited success as a high-volume replacement.⁽³⁾

In response to this issue, a research team conducted a study called “Physically Informed Data-Driven Methods for Greatly Enhancing the Use of Heterogeneous Supplementary Cementitious Materials in Transportation Infrastructure.” With an unprecedented massive concrete and FA dataset collection of 40,000 data records, the team conducted a series of experiments that used advanced material characterizations, machine-learning (ML) techniques, and numerical simulations to uncover the fundamental attributes governing the reactivity of FA and its suitability as a PC replacement. This work aimed to enhance the use of FA for producing more sustainable concrete.

Project Overview

The researchers broke down the project into a series of tasks that applied ML techniques to create analytical models that could predict the molecular characteristics and reactivity of FA, FA's interaction with PC, and the subsequent engineering properties of concrete containing FA.

SELECTING AND CHARACTERIZING PHYSICAL/CHEMICAL INDICATORS FOR THE REACTIVITY OF FA

The reactivity of FA's amorphous phase determines the ability of an FA to replace cement in concrete. But characterizing FA's amorphous phase is complex and cost prohibitive—which has thus far prevented any high-throughput screening of FAs to assess their suitability as SCMs. To better understand FA and its reactivity, the research team first developed an analytical model to predict the atomic topology of calcium (Ca) aluminosilicate (CAS) glasses. CAS is the essential component of the amorphous phase of both Class C (Ca-rich) and Class F (Ca-poor) FAs. This model was established based on topological constraint theory (TCT), which predicts various properties of oxide glasses as a function of their composition and structure.

TCT has been a key enabler in developing predictive models that relate the composition and structure of glasses to their properties.^(4,5) TCT simplifies complex disordered atomic networks into simpler nodes (the atoms) connected to each other by chemical bonds (their topological constraints). In structural glasses, topological constraints comprise the radial two-body bond stretching and angular three-body bond-bending constraints. The number of constraints per atom (nc) then offers a simple, reduced-dimensionality metric that is often correlated with macroscopic properties.⁽⁶⁾

To test this model, the researchers engaged in classical molecular dynamics simulations of 231 CAS glasses using the Large-Scale Atomic/Molecular Massively Parallel Simulator package.^(4,5,6) CAS glass samples were created using the conventional melt-quench method (a process of melting and cooling

the material). The glasses' molecular structure was then analyzed, and the atoms within each structure were labeled. The interaction of the various atoms within the molecular structure was also examined, especially areas that were Ca rich and aluminum rich. The subsequent model predicted the average topology of CAS glasses based on their composition. The model was used to determine the state of rigidity of CAS glasses based on their temperature and composition. This model yields the state of rigidity (flexible, isostatic, or stressed rigid) of CAS systems as a function of composition and temperature. These results reveal the existence of correlations between network topology and glass-forming ability—that is, the propensity for a liquid to form a disordered glass or an ordered crystal upon quenching. This experiment suggested that glass-forming ability is encoded in the network topology of the liquid state (i.e., during the quenching of the FAs from the liquid state) rather than that of the glassy state. This finding is important since both the state of rigidity of the atomic network of fly ashes and the fraction of the glassy phase therein govern their reactivity (i.e., their ability to dissolve and react in aqueous environments to contribute to the strength development in concrete).

Based on this understanding of the network topology of FA's glassy amorphous phase, the team developed a process for screening the reactivity of FAs based on fast, inexpensive bulk characterization called X-ray fluorescence (XRF). The researchers trained an artificial neural network (ANN) model (using a dataset of more than 100 FAs) that mapped out the bulk XRF composition of an FA to accurately predict the mass

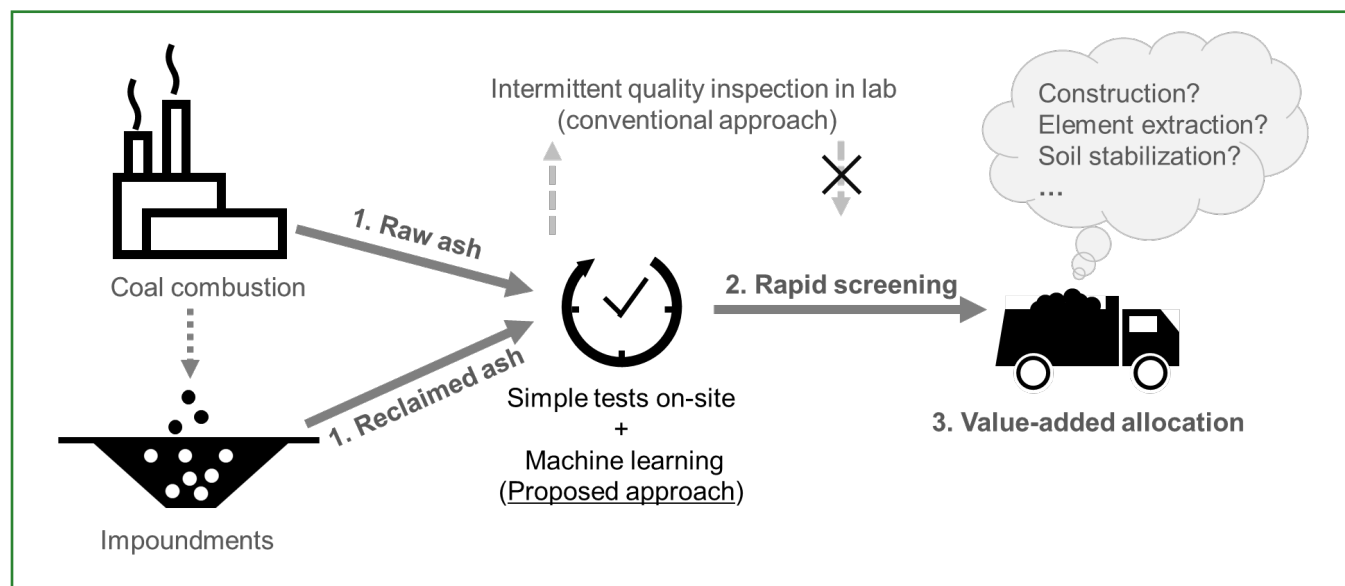
fraction of FA's amorphous phase and network topology. This new method could help maximize the beneficial use of FAs obtained from routine production as well as identify opportunities for the reclamation of ashes that are presently stored in impoundments. As figure 1 shows, easily measurable FA properties are mapped to key performance metrics to inform decisionmaking regarding which end usage should be preferred.

DEVELOP EXPERIMENTAL AND SYNTHETIC DATASETS TO TRAIN ML MODELS TO PREDICT THE ENGINEERING PROPERTIES OF [PC + FA] MIXTURES

The researchers developed a deep forest (DF) model to predict time- and composition-dependent hydration kinetics and compressive strength in relation to the mixture design of [PC + FA] binders and the physical and chemical properties of 10 FAs. The DF model was coupled with the segmentation technique (inserting different types of samples into specific segments during the training of the model) to enhance the prediction performance. Finally, through inference

of the intermediate and final outputs of the DF model, a simple, closed-form analytical model was developed to predict compressive strength and reveal the correlations between mixture design and compressive strength of [PC + FA] binders.

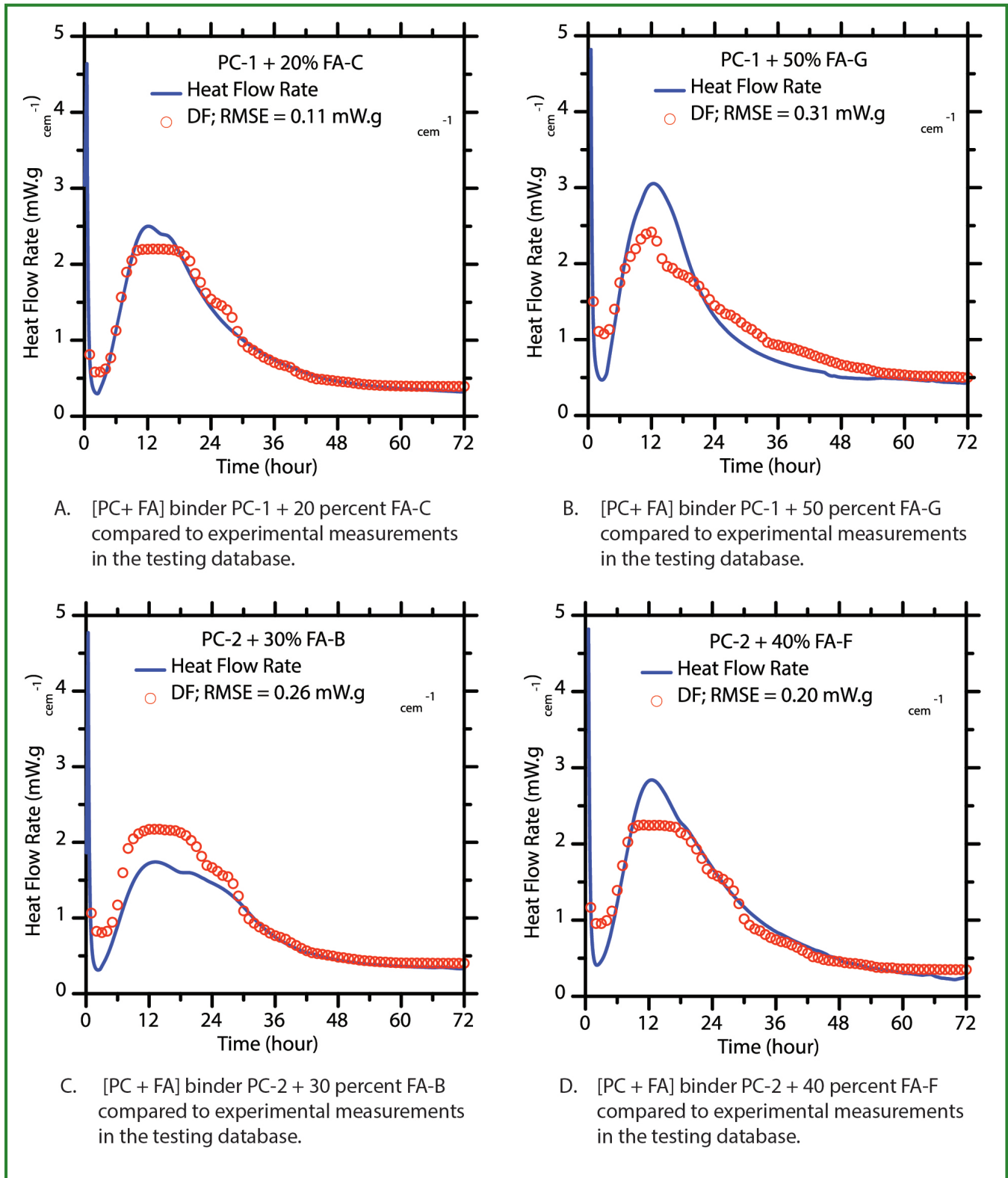
The researchers analyzed the chemical composition of obtained PC and FA, produced [PC + FA] concrete samples, and measured each sample's heat flow profiles of the [PC+FA] concrete binders. Heat-flow is the amount of heat following the hydration of PC that causes a temperature rise in cement. The researchers also measured the compressive strength of each sample. A random portion of the measured heat-flow profiles and compressive strength datapoints from the [PC + FA] concrete binders were input into a DF model. Five statistical parameters were employed to assess the performance of DF models on the testing datasets: mean absolute percentage error (*MAPE*), mean absolute error (*MAE*), Pearson correlation coefficient (*R*), root mean squared error (*RMSE*), and coefficient of determination (*R*²).



© 2021 American Chemical Society.

Figure 1. Schematic. Proposed ML-based screening approach.

Project Overview



© 2022 Missouri University of Science and Technology.

Figure 2. Graph. The standalone DF model predictions of heat-flow rate.

The DF model was used to predict heat-flow rate profiles of 10 randomly selected [PC + FA] binders every hour for a 72-h hydration period. Figure 2 shows predicted heat-flow rate profiles of representative [PC + FA] binders as produced by the standalone DF model against experimental measurements. To visually compare the predicted and measured values, the entire heat-flow rate spectrums are included. The statistical parameters pertaining to the prediction performance of the 72-h hydration period on the testing dataset are itemized in table 1.

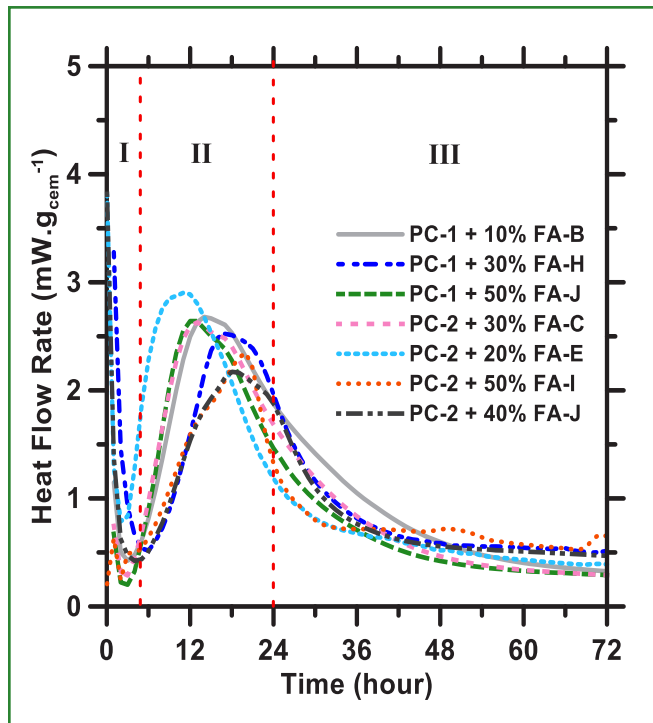
Due to the small-volume dataset (containing only 101 binders), the DF model was subsequently fine-tuned to reliably predict the heat-flow rate of FA. The team integrated a hydration theory-guided segmentation technique into the model to reduce the complexity of the database and enhance the model’s prediction accuracy. The segmentation technique is based on the hypothesis that, in the same segment, the hydration behavior of all [PC + FA] binders should be driven by the same mechanisms and, therefore, should manifest as similar kinetic (heat flow) profiles. The heat-flow rate was divided into three segments:

1. The first segment: The initial and induction periods (the first two stages of the hydration reaction—the chemical reaction in the concrete production process when water is added to cement). In this segment, high heat release is observed in the first hour, and the heat-flow rate for the remaining duration is low.
2. The second segment: The acceleration period (the third stage of the hydration reaction, when it is most intense).
3. The third segment: The deceleration period (the final stage of the hydration reaction, where the heat-flow rate diminishes).

3. The third segment: The deceleration period (the final stage of the hydration reaction, where the heat-flow rate diminishes).

The research team developed an algorithm to find the optimal thresholds for the segmentation. Figure 3 shows the thresholds for the different segments in representative binders.

After the [DF + Segmentation] model received the training dataset, the segmentation algorithm separated



© 2022 Missouri University of Science and Technology. Note: Based on their kinetic behaviors, the profiles are divided into three segments: initial and induction periods, acceleration period, and deceleration period.

Figure 3. Graph. Heat-flow rate profiles of randomly selected [PC+ FA] binders.

ML Model	<i>R</i> (Unitless)	<i>R</i> ² (Unitless)	<i>MAE</i> (mW g _{cem} ⁻¹)	<i>MAPE</i> (Percent)	<i>RMSE</i> (mW g _{cem} ⁻¹)
DF	0.9476	0.8981	0.1471	13.27	0.2463
DF + Segmentation	0.9743	0.9871	0.0701	7.43	0.1197

Table 1. Statistical parameters pertaining to the prediction performance of DF and [DF + Segmentation] models on 72-h heat-flow rate.

Project Overview

the training dataset into three sub-datasets. Then, three parallel DF models were independently trained with three sub-datasets to find the input-output correlations for each segment. When a testing dataset was implemented into the model, three parallel DF models predicted the heat-flow rate of [PC + FA] binders with respect to their segments. Later, the segmentation algorithm combined the outcomes from DF models to produce the entire heat-flow rate profile. Table 1 illustrates the improved predictive power of the DF model integrated with the segmentation algorithm.

For predicting binder compressive strength, the team first tested the compressive strength of binder cube specimens, [PC-1 + FA] and [PC-2 + FA]. These measurements were compared to predictions based on the DF model that was trained with a database of compressive strength from 92 unique [PC + FA] binders (i.e., 2 plain PCs and 90 PCs replaced by FAs). As shown in figure 4 and table 2, predictions of compressive strength against the testing dataset are reliable, with R^2 and $RMSE$ being 5.22 MPa. The typical measurement error of compressive strength is 5 MPa, where the prediction error is close to the experimental error.⁽⁷⁾

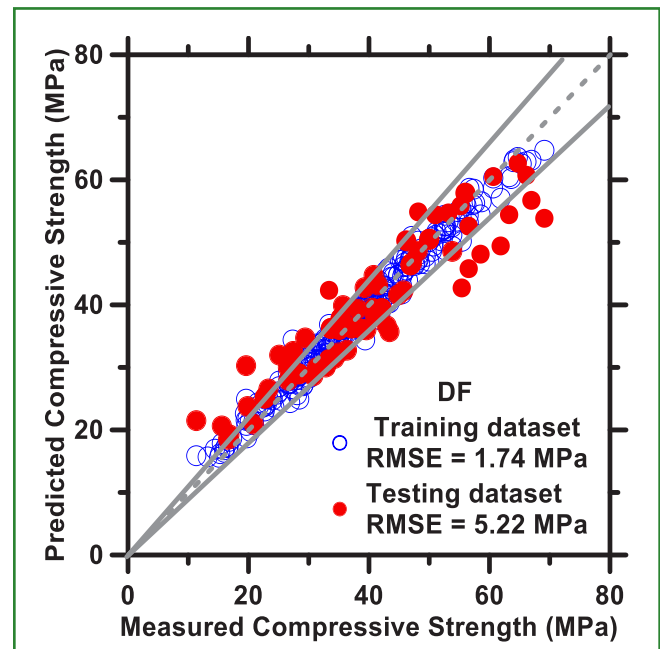
DEVELOP A SET OF ML MODELS TO OPTIMIZE AND PREDICT THE PERFORMANCE OF [PC + FA] MIXTURES

Predicting Concrete's Strength by ML Balance Between Accuracy and Complexity of Algorithms

The team leveraged a dataset (comprising 10,264 observations) of measured compressive strength

values obtained from actual job-site concrete mixtures and their corresponding mixture proportions.⁽⁸⁾ The reported mixture proportions reflected the actual mixture proportions, i.e., based on the batch weights of industrially produced concretes that were either truck- or central-plant mixed. Furthermore, all the strength measurements reported in the datasets used ASTM C150-compliant Type I/II PC. Class F FA compliant with ASTM C618 was used in select cases.^(9,10)

The team conducted a permutation importance analysis to select the concrete characteristics in the



© 2022 Missouri University of Science and Technology. Note: The dashed line is the ideal prediction. The solid lines are ± 10 percent error bounds.

Figure 4. Graph. The predictions of compressive strength of [PC + FA] binders as produced by the DF model against the testing dataset.

ML Model	R (Unitless)	R^2 (Unitless)	MAE (MPa)	MAPE (Percent)	RMSE (MPa)
DF	0.9368	0.8775	3.939	11.34	5.221
Analytical model	0.9031	0.8156	4.051	11.6	5.322

Table 2. The statistical parameters pertaining to the prediction performance of the DF and analytical models on [PC + FA] binders' compressive strength.

datasets to be used as inputs for the ML models considered.⁽¹¹⁾ This analysis (conducted based on the ANN model) randomly shuffled each characteristic and tracked the associated loss in accuracy to determine which characteristics were most important. As shown in figure 5, the six most influential characteristics controlling concrete’s strength were (in order of decreasing importance):

1. Water-to-cement ratio (w/c, mass basis).
2. Fine aggregate mass fraction.
3. Water-reducing admixture (WRA) dosage.
4. Coarse aggregate mass fraction.
5. FA mass fraction.
6. Air-entraining admixture (AEA) dosage.

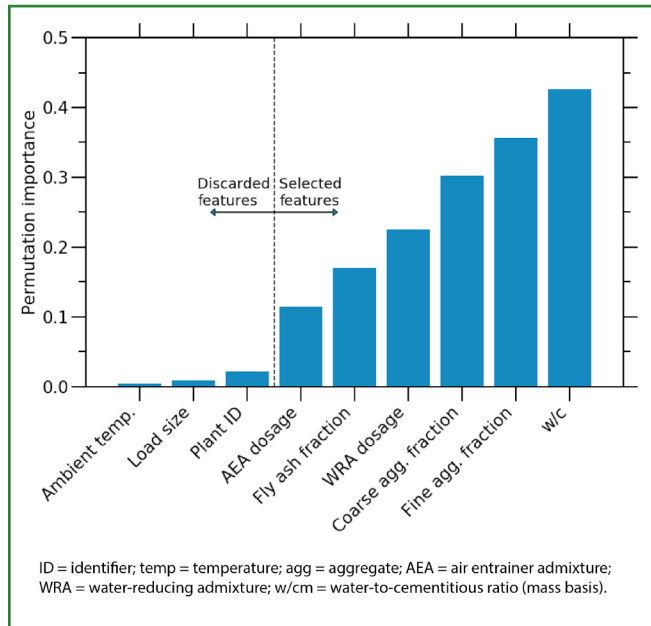
Once the important characteristics were identified, the researchers employed multiple ML methods:

- Polynomial regression.
- ANN.
- Random forest.
- Boosted tree.

The researchers then tested the accuracy of each of these ML models, finding that they all predicted the compressive strength of [PC + FA] concrete well. Random forest, in particular, provided the most optimal balance between accuracy, complexity, and interpretability.

Using ML to Predict Concrete’s Strength: Learning from Small Datasets

The researchers also conducted a study using ML techniques to predict [PC + FA] concrete’s compressive strength with a smaller dataset. The dataset used in this study comprises the 28-d compressive strength of 10,264 commercial concretes and their associated mixture proportions.⁽⁸⁾ All the mixtures were cast using ASTM C150-compliant



© 2022 University of California, Los Angeles.

Figure 5. Graph. Permutation importance of each of the features considered.

Type I/II cement and Class F FA compliant with ASTM C618, where FA is a by-product of coal power plants that can be used as SCM to replace cement in concrete.^(12,13,14) The seven most influential features were considered in this study:

1. W/c ratio (in this case, the ratio between the mass of water and that of cement and FA).
2. Cement fraction.
3. FA fraction.
4. Fine aggregate fraction.
5. AEA dosage (used for enhancing concrete durability).
6. WRA dosage (used for increasing concrete early-stage workability).

For normalization purposes, features 2–4 were considered solid-weight fractions. The fraction of coarse aggregates was excluded as it was the same as features 2–4.

The team used 70 percent of the strength observations from its dataset as a model training for three ML algorithms (polynomial regression, ANN, and random forest). They then evaluated the accuracy of each model based on its *RMSE* and coefficient of determination. Each model's learning efficiency—how each model learns how to predict concrete strength as it is exposed to increasing numbers of training examples—was also evaluated. Since the dataset for this study was relatively small, the researchers assessed the ability to make generalizations based on each model.

Interpreting the Strength Activity Index (SAI) of FA with ML

To promote the use of high-volume FA in concrete, the researchers used ML methods to infer the SAI of FAs.

SAI is an indicator of the quality of additional materials mixed into cement when producing concrete. Leveraging a dataset comprising 2,158 FA samples, the researchers trained ANN models to predict 28-d SAI based on the sole knowledge of ASTM C618 material attributes.⁽¹³⁾ The ANN model could accurately predict the 28-d SAI, where the prediction error averaged on the testing samples is merely 2.2 percent. The results demonstrated that SAI is a complex property that does not systematically follow the conventional Class C/F classification. To gain a deeper insight into this matter, the team further quantified the influence of each attribute on SAI as captured by the ML model.

Conclusions

Overall, the results of this study demonstrated the ability of ML techniques to help better understand FA and predict its interaction with cement to create concrete and the concrete mixture's subsequent engineering properties.

The researchers found that by examining CAS glass and its molecular structure as a proxy, they could develop a model for FA that could predict its reactivity potential. This work can help facilitate the mass use of FA to create more sustainable concrete by enabling screening using XRF. Bulk screening can help decipher which FA would be most suitable for concrete production.

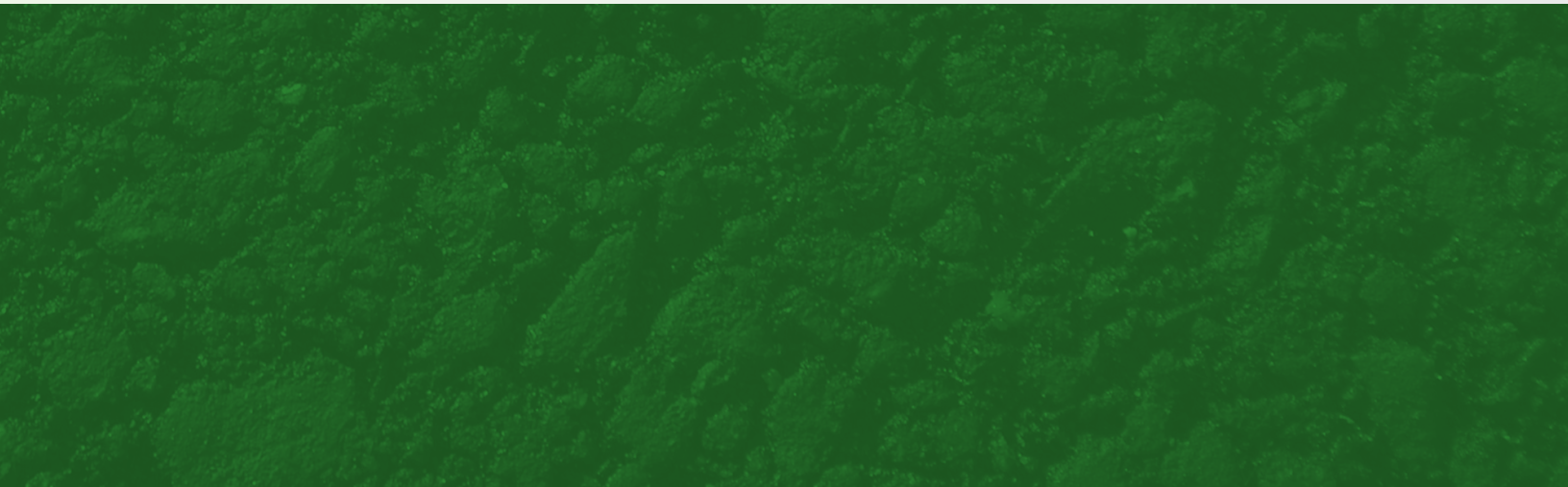
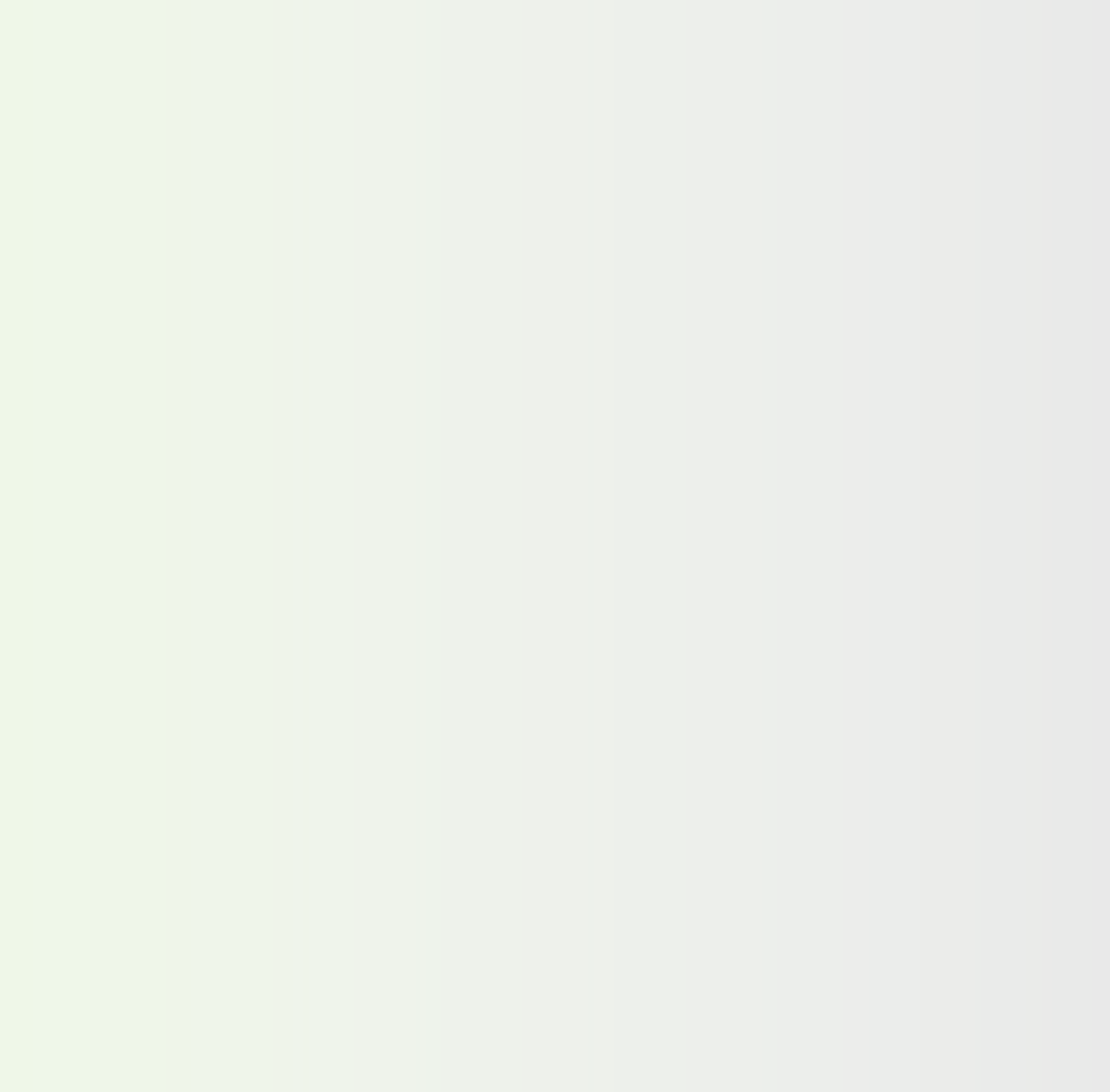
In addition, from the work of this research team, the interaction of FA and cement, the [PC + FA]

binders, and their compressive strength could be predicted using the DF model. The researchers demonstrated that this result could be accomplished with a limited dataset.

The results from the SAI test were the first time that an ML model was successfully used for predicting SAI. In addition, by implementing a model interpretation technique, the researchers further decoded the black-box ANN model. The team also found how the individual material attributes synergistically determine SAI. From a practical perspective, the accurate prediction of SAI can significantly promote the optimal use of FA for sustainable concrete construction.

REFERENCES

1. Ulm, F. -J. 2012. "Nano-Engineering of Concrete." *Arabian Journal for Science and Engineering* 37, 481. <https://doi.org/10.1007/s13369-012-0181-x>, last accessed January 31, 2023.
2. Van Ruijven, B. J., Van Vuuren, D. P., Boskaljon, W., Neelis, M. L., Saygin, D., and M. K. Patel. 2016. "Long-Term Model-Based Projections of Energy Use and CO₂ Emissions from the Global Steel and Cement Industries." *Resources, Conservation and Recycling* 112, 15. <https://doi.org/10.1016/j.resconrec.2016.04.016>, last accessed January 31, 2023.
3. Juenger M. C. G., F. Winnefeld, J. L. Provis, and J. H. Ideker. 2011. "Advances in Alternative Cementitious Binders." *Cement and Concrete Research* 41, 1232–1243. <https://doi.org/10.1111/jace.14974>, last accessed January 31, 2023.
4. Phillips, J. C. 1979. "Topology of Covalent Non-Crystalline Solids I: Short-Range Order in Chalcogenide Alloys." *Journal of Non-Crystalline Solids* 34, 153–181. [https://doi.org/10.1016/0022-3093\(79\)90033-4](https://doi.org/10.1016/0022-3093(79)90033-4), last accessed January 31, 2023.
5. Thorpe, M. F. 1983. "Continuous Deformations in Random Networks." *Journal of Non-Crystalline Solids* 57, 355–370. [https://doi.org/10.1016/0022-3093\(83\)90424-6](https://doi.org/10.1016/0022-3093(83)90424-6), last accessed January 31, 2023.
6. Bauchy, M. 2019. "Deciphering the Atomic Genome of Glasses by Topological Constraint Theory and Molecular Dynamics: A Review." *Computational Materials Science* 159, 95–102.
7. Hu, Y. -J., G. Zhao, M. Zhang, B. Bin, T. Del Rose, Q. Zhao, Q. Zu, Y. Chen, X. Sun, M. De Jong, and L. Qi. 2020. "Predicting Densities and Elastic Moduli Of SiO₂-Based Glasses By Machine Learning." *npj Computational Materials* 6, 1–13. <https://doi.org/10.1038/s41524-020-0291-z>, last accessed January 31, 2023.
8. Zanotto, E. D., and F. A. B. Coutinho. 2004. "How Many Non-Crystalline Solids Can Be Made From All the Elements of the Periodic Table?" *Journal of Non-Crystalline Solids* 347, 285–288. <https://doi.org/10.1016/j.jnoncrysol.2004.07.081>, last accessed January 31, 2023.
9. Liu, H., T. Du, N. M. A. Krishnan, H. Li, and M. Bauchy. 2019. "Topological Optimization of Cementitious Binders: Advances and Challenges." *Cement and Concrete Composites* 101, 5–14. <https://doi.org/10.1016/j.cemconcomp.2018.08.002>, last accessed January 31, 2023.
10. Nawy, E. G., ed. 2008. *Concrete Construction Engineering Handbook*. Boca Raton, FL: CRC Press.
11. Young, B. A., A. Hall, L. Pilon, P. Gupta, and G. Sant. 2019. "Can the Compressive Strength of Concrete Be Estimated From Knowledge of the Mixture Proportions?: New Insights From Statistical Analysis and Machine Learning Methods." *Cement and Concrete Research* 115, 379–388.
12. ASTM International. 2018. *Standard Specification for Portland Cement*. ASTM C150/C150M-17. West Conshohocken, PA: ASTM International.
13. ASTM International. 2010. *Standard Specification for Coal Fly Ash and Raw or Calcined Natural Pozzolan for Use in Concrete*. ASTM C618-08a. West Conshohocken, PA: ASTM International.
14. Conn, R. E., K. Sellakumar, and A. E. Bland. 1999. *Utilization of CFB Fly Ash for Construction Applications*. Presented at the 15th International Conference on Fluidized Bed Combustion. Savannah, GA: U.S. Department of Energy Office of Scientific and Technical Information.



Getting Involved with the EAR Program

To take advantage of a broad variety of scientific and engineering discoveries, the EAR Program involves both traditional stakeholders (State department of transportation researchers, University Transportation Center researchers, and Transportation Research Board committee and panel members) and nontraditional stakeholders (investigators from private industry, related disciplines in academia, and research programs in other countries) throughout the research process.

EXPLORATORY ADVANCED RESEARCH



Recommended citation: Federal Highway Administration, *Physically Informed Data-Driven Methods for Greatly Enhancing the Use of Heterogeneous Supplementary Cementitious Materials in Transportation Infrastructure* (Washington, DC: 2023) <https://doi.org/10.21949/1521984>



U.S. Department of Transportation
Federal Highway Administration

FHWA-HRT-23-040
HRTM-30/07-23(WEB)E